Acta Cryst. (1996). B**52**, 954–960

A Re-examination of the Relationship Between Lattice Strain, Octahedral Tilt Angle and Octahedral Strain in Rhombohedral Perovskites

NOEL W. THOMAS

School of Materials, University of Leeds, Leeds LS2 9JT, England. E-mail: n.w.thomas@leeds.ac.uk

(*Received 12 March 1996; accepted 8 July 1996*)

Abstract

A new expression is proposed for the relationship between lattice strain $90° - \alpha_{pc}$ (α_{pc}: pseudo-cubic angle) and mean BO_6 octahedral tilt angle $<\omega>$ in rhombohedral perovskites ABO_3. It is derived from volumetric arguments, leading to a cubic equation which incorporates lattice strain $90° - \alpha_{pc}$ and octahedral elongation explicitly. Numerical solutions of this equation are derived for equally spaced values of octahedral strain, giving rise to a set of parametric curves which relate ω to $90° - \alpha_{pc}$ for different values of η. These curves can be represented as polynomials of the fourth degree, thereby enabling their routine use in the analysis of rhombohedral perovskite structures. It is anticipated that these parametric curves will supersede earlier work [Megaw & Darlington (1975). *Acta Cryst.* A**31**, 161–173], in which an analytical expression was derived linking $90° - \alpha_{pc}$, ω and octahedral strain for positive lattice strains only. By comparison, the relationship proposed here accommodates both negative and positive lattice strains. Correlations between values of $<\omega>$, η, $90° - \alpha_{pc}$ and space-group symmetry are found, with an analysis of known rhombohedral and orthorhombic *Pnma* structures revealing the importance of cationic charges in determining symmetry. Since the polyhedral volume ratio V_A/V_B may be quantitatively related to $<\omega>$, allowed values of tilt angle, lattice strain and octahedral elongation may be inferred for a given composition, which has characteristic values of V_A and V_B.

1. Introduction

The relationship between lattice strain and octahedral tilt angle in rhombohedral perovskites, ABO_3, has been the subject of two previous studies. In the first of these (Michel, Moreau & James, 1971), the structures of perovskites in space group $R\bar{3}c$ were modelled, with the assumption of rigid BO_6 octahedra. This permitted the octahedral tilt angle ω to be related to departures of the rhombohedral angle α_{rh} from 60° to lower values. The second study (Megaw & Darlington, 1975) extended the structural parameterization to include deviations of the BO_6 octahedra from regularity. Two possible components were identified: (i) differences in facial areas of the two octahedral triangular faces perpendicular to the triad axis; (ii) elongations or compressions of the octahedra parallel to this axis.

The inter-relationship of rhombohedral, hexagonal and pseudo-cubic axes was also articulated in the paper by Megaw & Darlington (1975), from which Fig. 1 is reproduced. Although the conventional unit cell for rhombohedral perovskites in space groups $R\bar{3}c$ and $R3c$ has a rhombohedral angle close to 60°, it was found expedient to utilize a pseudo-cubic rhombohedral cell instead, for which $\alpha_{pc} \simeq 90°$. These authors went on to derive the following relationship between pseudo-cubic rhombohedral angle α_{pc} and tilt angle ω

$$\cos\alpha_{pc} = [\sin^2\omega/(3 - 2\sin^2\omega)] + \{(2/3)\zeta/[1 - (2/3)\sin^2\omega]\}. \quad (1)$$

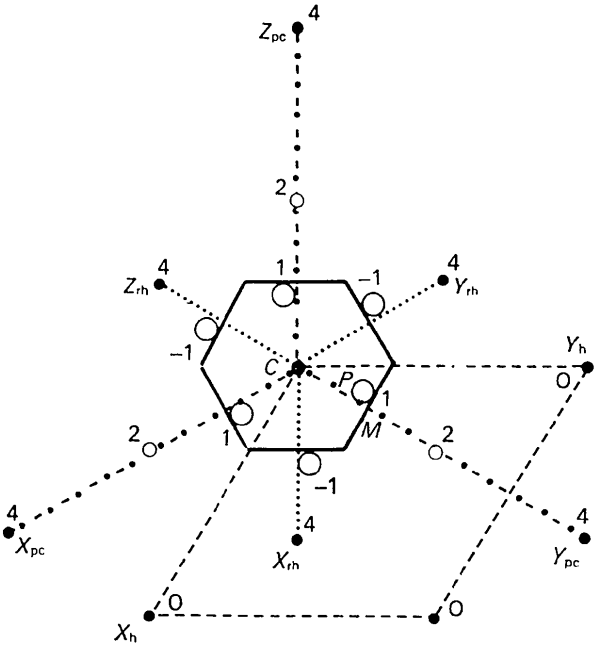

Fig. 1. Relationship between hexagonal (dashed), pseudo-cubic (dot–dash) and primitive rhombohedral (dotted) unit cells. Projection is down the triad axis; heights are in units of $c_H/12$. Small black circles are lattice points for $R\bar{3}c$ and $R3c$, corresponding to corners of a rhombohedral unit cell with α close to 60°; small open circles are octahedral centres forming corners of a pseudo-cubic rhombohedral unit cell with α close to 90°. Large open circles are O atoms, forming a slightly distorted octahedron about the B cation situated nearest the origin (courtesy of Megaw & Darlington, 1975).

where ζ represents octahedron strain parallel to the triad axis. Elongated octahedra would have $\zeta > 0$, with ζ values less than zero signifying compression. The form of this variation is plotted in Fig. 2, for the case of unstrained octahedra ($\zeta = 0$). The concept of a lattice strain, $90° - \alpha_{pc}$, is introduced in the figure, representing the extent of the deviation of the pseudo-cubic angle α_{pc} from 90°. Whereas the solid line has a theoretical basis in the first term in (1), this is not the case for the dashed line, which has been constructed empirically from experimental points 4, 5, 6 and 7.

The aim of the present paper is to re-examine the relationship between ω and α_{pc} for rhombohedral perovskites. In particular, the theoretical dependence of ω on $90° - \alpha_{pc}$ will be derived for negative lattice strains, thus replacing the empirical curve of Megaw & Darlington (1975). It will be seen that the predicted dependence is at variance with their empirical curve (Fig. 2).

2. Derivation of relationships between octahedral tilt angle ω, lattice strain $90° - \alpha_{pc}$ and octahedral strain η

2.1. *Equation linking α_{pc} and c_H/a_H*

The pseudo-cubic rhombohedral angle α_{pc} is related to the volume of the pseudo-cubic cell by the following variation (see, for example, Hammond, 1990)

$$V_{u,pc} = a_{pc}^3(1 - 3\cos^2\alpha_{pc} + 2\cos^3\alpha_{pc})^{1/2}, \qquad (2)$$

where a_{pc} is the pseudo-cubic cell constant. As shown in Fig. 1, lattice points of the pseudo-cubic cell are at a height $c_H/3$, with their projections in the X_hY_h plane at distances $2a_H/3^{1/2}$ from the origin. Furthermore, the volume of the pseudo-cubic cell is 4/3 the volume of the hexagonal unit cell,* *i.e.*

$$[(2a_H/3^{1/2})^2 + (c_H/3)^2]^{3/2}(1 - 3\cos^2\alpha_{pc} + 2\cos^3\alpha_{pc})^{1/2} = 4V_{u,H}/3. \qquad (3)$$

Since $V_{u,H} = a_H^2 c_H 3^{1/2}/2$, it follows that

$$(1 - 3\cos^2\alpha_{pc} + 2\cos^3\alpha_{pc})^{1/2} = 2a_H^2 c_H/\{3^{1/2}[(2a_H/3^{1/2})^2 + (c_H/3)^2]^{3/2}\},$$

which simplifies to

$$1 - 3\cos^2\alpha_{pc} + 2\cos^3\alpha_{pc} = 36a_H^4 c_H^2/(4a_H^2 + c_H^2/3)^3. \qquad (4)$$

Of particular interest here is the ratio c_H/a_H, since this has a direct bearing on the octahedral strain parallel to the triad axis. Let this ratio be denoted by r, so that (4) becomes

$$1 - 3\cos^2\alpha_{pc} + 2\cos^3\alpha_{pc} = 36r^2/(4 + r^2/3)^3. \qquad (5)$$

2.2. *Solution of equation (5)*

The value of r for any given value of α_{pc} is calculated by evaluating the left-hand side of (5) and representing the result as λ. Thus, $\lambda(4 + x/3)^3 = 36x$, where $x = r^2$. On expansion and rearrangement this becomes

$$(\lambda/27)x^3 + (4\lambda/3)x^2 + (16\lambda - 36)x + 64\lambda = 0. \qquad (6)$$

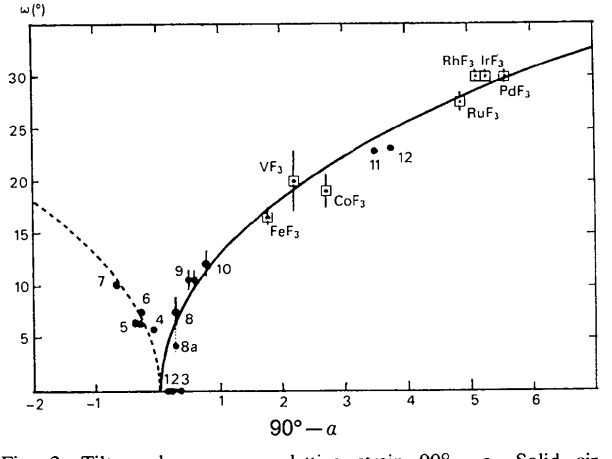

Fig. 2. Tilt angle ω *versus* lattice strain $90° - \alpha$. Solid circles are experimental points for the following compounds: (1) $BaTiO_3$ (183 K); (2) $KNbO_3$ (230 K); (3) $Pb(Zr_{0.58}Ti_{0.42})O_3$; (4) $LaAlO_3$; (5) $PrAlO_3$; (6) $BaTbO_3$; (7) $LaCoO_3$; (8) and (8*a*) $Pb(Zr_{0.90}Ti_{0.10})O_3$; (9) $BiFeO_3$; (10) $NaNbO_3$ (N phase); (11) $LiTaO_3$; (12) $LiNbO_3$. The full line, for $90° - \alpha > 0$, is given by the first term in equation (1), *i.e.* when octahedron strain $\zeta = 0$. The dashed line is an empirical curve, constructed by reflecting the full line at $90° - \alpha$ (courtesy of Megaw & Darlington, 1975).

* This can also be inferred from the observation that $Z_H = 6$, whereas $Z_{pc} = 8$.

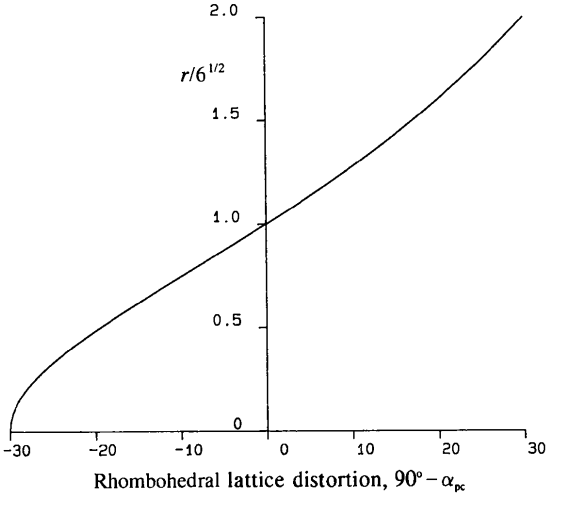

Fig. 3. Variation of axial ratio $r = c_H/a_H$ with lattice strain, $90° - \alpha_{pc}$, as predicted by equation (5).

Equation (6) can be solved numerically, by means of an appropriate algorithm.* Only one of the three roots of x obtained for a given value of λ corresponds to the physically correct solution. Since $r = x^{1/2}$, any solution for x must be real and positive. Further criteria for selecting the correct root depend on the value of α_{pc}, which affects the ratio of the c_H and a_H parameters directly. When $\alpha_{pc} = 90°$, $r = c_H/a_H = 6^{1/2}$ and $x = 6$; when $\alpha_{pc} < 90°$, $r = c_H/a_H > 6^{1/2}$, so that $x > 6$; when $\alpha_{pc} > 90°$, $r = c_H/a_H < 6^{1/2}$, so that $x < 6$.

The computed variation of r with lattice strain $90° - \alpha_{pc}$ is shown in Fig. 3, for values of $90° - \alpha_{pc}$ between -30 and $+30°$. For $90° - \alpha = -30°$, *i.e.* $\alpha_{pc} = 120°$, $r = 0$, in agreement with a unit-cell volume of zero, as predicted by (2). For $90° - \alpha_{pc} = +30°$, $r = 2(6)^{1/2}$, with $r = 6^{1/2}$ when $90° - \alpha_{pc} = 0$. It is to be noted that the variation of r with $90° - \alpha_{pc}$ approximates to a straight line in the region near $90° - \alpha_{pc} = 0$. The best-fit straight line for $90° - \alpha_{pc}$ values in the range -8 to $+8°$ has been determined to be $r/6^{1/2} = 1.0036 + 0.026418(90° - \alpha_{pc})$. A more accurate quadratic fit gives $r/6^{1/2} = 1.0000 + 0.026358(90° - \alpha_{pc}) + 0.00011333(90° - \alpha_{pc})^2$. (Residuals for these fits from the NAG routine E02ACF amount to 0.00369 and 0.00048, respectively.)

*For example, NAG Fortran Subroutine Library, routine C02AEF NAG Ltd, Wilkinson House, Jordan Hill Road, Oxford OX2 8DR, England.

2.3. *Dependence of a_H on octahedral tilt angle, ω*

A parameterization for quantifying octahedral tilt angles in rhombohedral perovskites has been previously defined by the author (Thomas & Beitollahi, 1994). Tilting is shown in Fig. 4(*a*) for the simplified case where all octahedral edge lengths are equal and in Fig. 4(*b*) for the general case of unequal edge lengths. In this

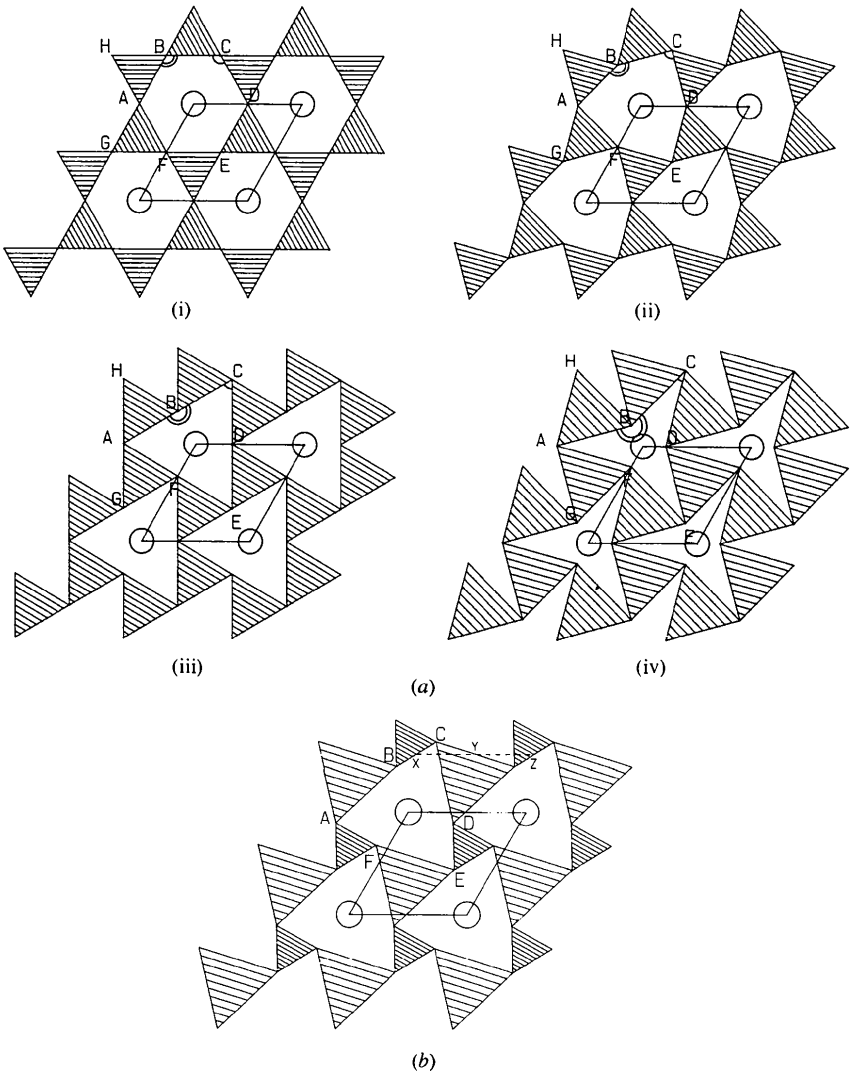

Fig. 4. (*a*) Projections of the rhombohedral perovskite structure viewed along the z direction in hexagonal axes: (i) $\omega = 0°$; (ii) $\omega = 15°$; (iii) $\omega = 30°$; (iv) $\omega = 45°$. The triangles represent co-planar faces of the BO_6 octahedra, which lie in the xy plane; A ions are represented as circles at the corners of the hexagonal unit cell, with the edge lengths of all triangles equal. In diagrams (ii), (iii) and (iv), triangle AGF is rotated by $+\omega$ about its centre and triangle ABH by $-\omega$ with respect to the 0° orientations in diagram (i). Thus, angle $BCD = 120° - 2\omega$ and $ABC = 120° + 2\omega$. The structure depicted in diagram (iv) is not found in practice, since this is associated with concave A-ion coordination polyhedra ($ABCDEF$, in projection). Thus, there is an upper limit of $\omega = 30°$, as shown in diagram (iii). (*b*) Sketch of the structure for an arbitrary tilt angle, with BO_6 octahedra of unequal edge lengths. The straight line XYZ (of length equal to the lattice constant a_H) links mid-points of the sides of three triangles with the angles within triangle XYC defining tilt angles α and β, such that $\langle\omega\rangle = (\alpha + \beta)/2$.

earlier work it was found expedient to use the equation $a_H = 2Ks\cos\langle\omega\rangle$ to relate a_H with the mean octahedral edge length s (in planes such as in Fig. 4*b*, perpendicular to the threefold axis) and mean tilt angle $\langle\omega\rangle$. The latter is derived by calculating values of angles *ABC* and *BCD* in Figs. 4(*a*) and (*b*), such that $\langle\omega\rangle = (ABC - BCD)/4$. It was found by examination of experimental crystal structures that the parameter K could be taken as 1.0000, to an excellent approximation, *i.e.*

$$a_H = 2s\cos\langle\omega\rangle. \quad (7)$$

2.4. *The influence of octahedral strain on c_H*

The term 'octahedral strain' has a restricted interpretation, either as an elongation or as a flattening of the octahedra in the direction parallel to the threefold axis (Megaw & Darlington, 1975). It is not to be confused with the existence of unequal octahedral edge lengths in planes perpendicular to the trigonal axis, as in Fig. 4(*b*). In the special case of regular octahedra (*i.e.* all edges of equal length), it may be shown that $h = (2/3)^{1/2}s$, where s is the octahedral edge length and h the face-to-face height along a threefold axis.* In the general case, therefore, h may be made equal to $(2/3)^{1/2}s\eta$. When $\eta > 1$, an octahedron is elongated, whereas a flattened octahedron would have $\eta < 1$. Note that $\eta = 1 + \zeta$, the parameter ζ having been introduced by Megaw & Darlington (1975) to denote octahedron strain. It follows from the geometry of the hexagonal unit cell that $c_H = 6h$, *i.e.*

$$c_H = 2(6)^{1/2}s\eta. \quad (8)$$

2.5. *Derivation of the relationship between $\langle\omega\rangle$, $90° - \alpha_{pc}$ and η*

Equations (7) and (8) may be combined to give

$$r = c_H/a_H = 6^{1/2}\eta/\cos\langle\omega\rangle. \quad (9)$$

Substitution of this result for r in (5), together with the notation $\delta = 90° - \alpha_{pc}$ for lattice strain, gives the following result

$$1 - 3\sin^2\delta_{pc} + 2\sin^3\delta_{pc} = 27\eta^2\cos^4\langle\omega\rangle/(2\cos^2\langle\omega\rangle + \eta^2)^3. \quad (10)$$

The validity of this equation may be checked by considering the particular case of $\eta = 1$. For all physically meaningful values of $\langle\omega\rangle$ (*i.e.* $\langle\omega\rangle \leq 30°$), the right-hand side is less than one, implying, from a consideration of the left-hand side, positive values of δ_{pc}. This can be interpreted geometrically as follows: any tilting of the octahedra leads to contraction of the hexagonal a axis and a reduced relative projected area of the AO_{12} coordination polyhedron. Since the length of the c axis is unaffected by the tilting, however, $\alpha_{pc} < 90°$ and $\delta_{pc} = 90° - \alpha_{pc} > 0$.

2.6. *Solutions of equation (10)*

Equation (10) indicates that lattice strain δ_{pc} is a function of both octahedral tilt angle $\langle\omega\rangle$ and octahedral strain η. Thus, solutions of this equation are best represented by a set of parametric curves for different η values. In order to derive these curves, the following procedure has been adopted.

Values of r were computed for equally spaced values of δ_{pc} between -8 and $+8°$, by use of (5). For each value of r, a set of 21 values of $\langle\omega\rangle$ was calculated, corresponding to equally spaced octahedral strains, $\eta = 0.95, 0.955, 0.960, \ldots, 1, \ldots, 1.05$. Since, from (9), $\langle\omega\rangle = \cos^{-1}(6^{1/2}\eta/r)$, values of $6^{1/2}\eta/r$ greater than one give no solution for $\langle\omega\rangle$. Eleven of these parametric curves are shown in Fig. 5, with small squares representing the experimentally determined perovskite structures analysed in a previous article (Thomas & Beitollahi, 1994).

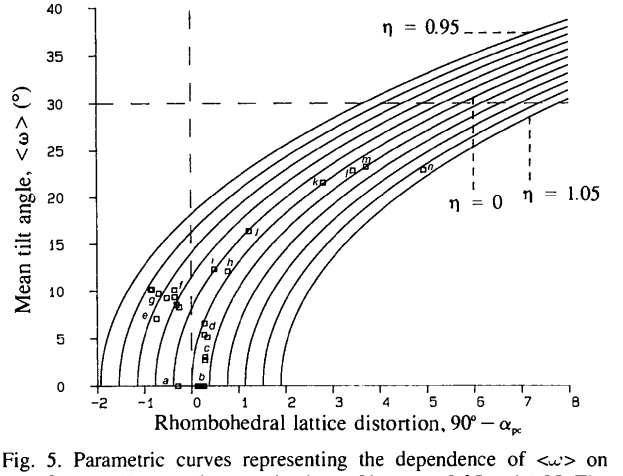

Fig. 5. Parametric curves representing the dependence of $\langle\omega\rangle$ on $90° - \alpha_{pc}$ for equally spaced values of between 0.95 and 1.05. The small squares, which represent experimental structures previously analysed (Thomas & Beitollahi, 1994), correspond to the following compositions: (*a*) $PrAlO_3$; (*b*) $Pb(Zr_xTi_{1-x})O_3$ *R3m* structures; (*c*) $Pb(Zr_{0.75}Ti_{0.25})O_3$ *R3c* structures; (*d*) $Pb(Zr_{0.9}Ti_{0.1})O_3$ *R3c* structures; (*e*) $LaCuO_3$; (*f*) $NdAlO_3$ (two structures); (*g*) $LaCoO_3$ (six structures; 4–1248 K); (*h*) $NaNbO_3$ (123 K); (*i*) $BiFeO_3$; (*j*) $HgTiO_3$; (*k*) $LiReO_3$; (*l*) $LiTaO_3$; (*m*) $LiNbO_3$; (*n*) $LiUO_3$. The horizontal dashed line represents the upper limit for physically realistic $\langle\omega\rangle$ values (see Fig. 4*a*). The vertical dashed line, which passes through $90° - \alpha_{pc} = 0$, separates non-polar structures on its left-hand side from polar *R3c* to its right. $R\bar{3}m$ and *R3m* structures, for which $\langle\omega\rangle = 0$, lie on the horizontal axis. All points for $R\bar{3}c$ and *R3c* structures, which have tilted octahedra, are displaced from this axis.

* A number of methods may be used to derive this result, for example, one based on octahedral volumes. A regular octahedron has the same volume as two square pyramids, each of volume $\frac{1}{3}Ad$, where A is base area and d pyramidal height. Since $A = s^2$ and $d = s/2^{1/2}$, octahedral volume $V_{oct} = 2^{1/2}s^3/3$. The dependence of h on s is derived from the result that the volume of an octahedron is also equal to $3^{1/2}d/12\,(A + B)^2$, where A and B are edge lengths of two parallel faces and d their separation (Thomas & Beitollahi, 1994). For a regular octahedron, $A = B = s$ and $d = h$, so that $V_{oct} = hs^2/3^{1/2}$. Equating this to $2^{1/2}s^3/3$ leads to the required result.

Table 1. *Values of polynomial coefficients a_{ij} to be substituted in equation (11)*

Subscript i	Subscript j 0	1	2	3
0	$-0.3885949 \times 10^{+2}$	$0.3383511 \times 10^{+2}$	$0.1071185 \times 10^{+2}$	$-0.5687345 \times 10^{+1}$
1	0.8425441×10^{-2}	$-0.2746044 \times 10^{-1}$	0.2824460×10^{-1}	$-0.9432612 \times 10^{-2}$
2	$-0.5884718 \times 10^{-2}$	0.2337373×10^{-1}	$-0.1517803 \times 10^{-1}$	0.3561531×10^{-2}
3	0.1171594×10^{-3}	$-0.3954808 \times 10^{-3}$	0.4120467×10^{-3}	$-0.1382055 \times 10^{-3}$
4	$-0.2618215 \times 10^{-5}$	0.1060686×10^{-4}	$-0.1062905 \times 10^{-4}$	0.3358051×10^{-5}

2.7. *Polynomial representations of the parametric curves*

Although the parametric curves in Fig. 5 are exact, their practical application requires expression in a form which does not require numerical solution of (5), which is a cubic equation. To this end, polynomials of the form $y = A + Bx + Cx^2 + Dx^3 + Ex^4$ have been fitted to the curves,* where y corresponds to $90° - \alpha_{pc}$ and x to $<\omega>$. The choice of a polynomial of degree 4 permits an acceptably good fit to the accurate curves of Fig. 5. Since the values obtained for coefficients A to E were found to vary monotonically with η, it was possible to derive further polynomial expansions for these coefficients in terms of η.* This latter procedure was carried out by calculating values for each of A, B, C, D and E for 21 equally spaced values of between 0.95 and 1.05. These were subsequently used to derive cubic polynomials with η as the independent variable. Thus, the full expression is as follows

$$90° - \alpha_{pc} = \sum_{j=0}^{j=3} a_{oj}\eta^j + \sum_{i=1}^{4}\left(\sum_{j=0}^{3} a_{ij}\eta^j\right) < \omega >^i \quad (0.95 \leq \eta \leq 1.05). \qquad (11)$$

The values of coefficients a_{ij} are given in Table 1, with the curves predicted by (11) plotted in Fig. 6 for $0 \leq <\omega> \leq 30°$.

* NAG Fortran Subroutine Library, routine E02ACF.

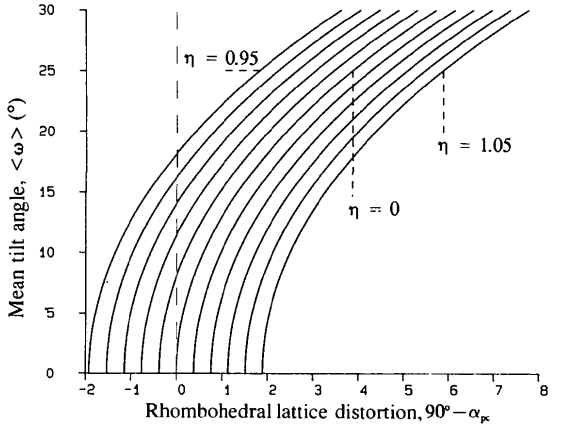

Fig. 6. Parametric curves derived from equation (11) with values of the polynomial coefficients given in Table 1.

3. Discussion

The set of parametric curves in Fig. 5 represents the variation of $<\omega>$ with lattice strain, $90° - \alpha$, for different octahedral strains, η. The analytical model of Megaw & Darlington (1975), obtained without the assistance of a digital computer, gave rise to a single curve only (Fig. 2), corresponding to $\eta = 1$. Agreement between their curve and the $\eta = 1$ curve of Fig. 5 is excellent for positive $90° - \alpha_{pc}$ values, to which their analysis refers. However, their construction of an 'empirical curve' for negative $90° - \alpha_{pc}$ values, obtained by reflection of the positive branch about $90° - \alpha_{pc} = 0$, is incorrect.

It is seen in Fig. 5 that a value of η of less than one is required for a given curve to pass through the region to the left of the y axis, in which $\alpha_{pc} > 90°$. Therefore, negative lattice strains (*i.e.* $\alpha_{pc} > 90°$) can only occur with compressed octahedra (*i.e.* $\eta < 1$). A further correlation is found by considering the experimental structures: those compositions with points to the right of the y axis crystallize in space groups $R3m$ and $R3c$, the two polar space groups. Thus, any rhombohedral perovskite which is ferroelectric will have a pseudo-cubic rhombohedral angle which is less than 90°. Conversely, all structures with points to the left of the y axis exist in the non-polar space groups $R\bar{3}m$ and $R\bar{3}c$.* As discussed previously (Thomas & Beitollahi, 1994), $R3c$ symmetry allows both octahedral tilting and unequal octahedral face areas perpendicular to the trigonal axis (Fig. 4*b*). The B ions are displaced towards the larger faces in polar structures. Freedom in the value of η is allowed, for example, this being less than one in $BiFeO_3$ and significantly greater than one in $LiUO_3$.

The relationship between ionic sizes and tilt angle $<\omega>$ in rhombohedral perovskites has been shown to correspond to the following equation (Thomas & Beitollahi, 1994)

$$V_A/V_B = 6\cos^2 < \omega > -1. \qquad (12)$$

Here, V_A/V_B is the ratio of the volume of the AX_{12} coordination cuboctahedron to that of the BX_6 octahedron, for a perovskite of general composition ABX_3. It has also been found that cations tend to adopt characteristic polyhedral volumes (Thomas, 1996). Thus,

* Space groups $R3m$ and $R\bar{3}m$ have points located on the x axis, since no octahedral tilting is permitted. By comparison, structures in space groups $R3c$ and $R\bar{3}c$ are represented by off-axis points, since their BO_6 octahedra are tilted (Thomas & Beitollahi, 1994).

to a good approximation, possible points for a given composition ABX_3 will lie somewhere on a horizontal line in Fig. 5, of fixed $<\omega>$ and therefore V_A/V_B value, its vertical height dictated by the sizes of A and B cations. In order to make the interdependence of $<\omega>$ and V_A/V_B explicit, the latter may also be plotted against $90° - \alpha_{pc}$ (Fig. 7), through the application of (11). It is seen that the parametric curves approximate to straight lines.

In structures with untilted octahedra, $V_A/V_B = 5$, falling to lower values as the tilt angle increases. However, a system with tilted octahedra does not necessarily have rhombohedral symmetry, since orthorhombic or tetragonal structures are also possible, for which $V_A/V_B = 6\cos^2\theta_m\cos\theta_z - 1$ (Thomas, 1996). Here, θ_m and θ_z are tilt angles defined relative to pseudo-cubic axes. Owing to this variation in octahedral tilt system, it is therefore appropriate to utilize the V_A/V_B ratio as an indicator of the degree of tilting, applicable to all perovskite structures, regardless of symmetry.

A mapping of known perovskite structures in space groups $R\bar{3}c$, $R3c$ and orthorhombic *Pnma* is given in Fig. 8, with V_A/V_B falling from 5 to 4 (*i.e.* tilting increasing) on the vertical axis and a division into three columns according to cationic charges, $A^{3+}B^{3+}O_3$[3,3], $A^{2+}B^{4+}O_3$ [2,4] or $A^{+}B^{5+}O_3$ [1,5]. Compressed octahedra (space group $R\bar{3}c$) are found only for [3,3]-perovskites with V_A/V_B values closest to 5. Within the [3,3] column, at $V_A/V_B \simeq 4.8$, there is a transition to an $R3c$ structure ($BiFeO_3$), with $\eta \simeq 0.990$. An $R\bar{3}c$ structure of identical V_A/V_B would have more compressed octahedra, *i.e.* ~ 0.975. A further reduction in V_A/V_B to 4.7 is associated with a change to orthorhombic symmetry (space group *Pnma*). Such an orthorhombic structure is to be regarded as an alternative to stabilization within a rhombohedral polar phase (space group $R3c$), which can tolerate smaller V_A/V_B values than its non-polar counterpart $R\bar{3}c$ (Fig. 7). The stabilization of $NdAlO_3$ and $BiFeO_3$ (points *a* and *b* in Fig. 8) in space group $R3c$ is probably best interpreted as a 'transitional symmetry' between $R\bar{3}c$ and *Pnma*. In adopting $R3c$ symmetry, the octahedral compression need not be as severe as would be the case in space group $R\bar{3}c$. It is also to be noted that the structure of $NdAlO_3$ has also been solved in space group $R\bar{3}c$ (point *e*), supporting the notion that $R3c$ symmetry is only transitional for [3,3]-perovskites. The $R\bar{3}c$–*Pnma* changeover is also of technological relevance to the current generation of ceramic fuel cells, which employ [3,3]-perovskites (Thomas, 1996).

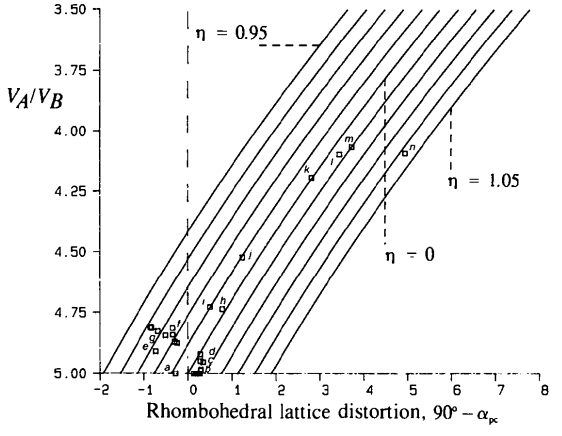

Fig. 7. Predicted relationship between V_A/V_B and $90° - \alpha_{pc}$ for equally spaced values of η between 0.95 and 1.05. The small squares correspond to experimentally determined structures, as defined in Fig. 5.

As discussed previously (Thomas, 1996), orthorhombic *Pnma* structures are characterized by closely coordinated B ions, with A ions displaced off-centre in an oversized AO_{12} environment. In $LuFeO_3$, for example, the Lu^{3+} ions are displaced by 0.4930 Å from their polyhedral centres, permitting a larger value of V_A than would otherwise be the case without this displacement. The corresponding energetic advantage of a larger AO_{12} polyhedron is a minimization of unfavourable O···O repulsions, which is clearly more important in [3,3]-perovskites than the adoption of an alternative, polar rhombohedral structure. This inference suggests that the dipole moments in [3,3]-perovskites are too weak to give rise to a strong dipolar contribution to the lattice energy. Indeed, there is evidence for a stronger dipolar contribution in [2,4]-perovskites, since structures with V_A/V_B close to 5 [*i.e.* $Pb(Zr_xTi_{1-x})O_3$ compositions] have polar $R3c$ in preference to non-polar $R\bar{3}c$ symmetry.

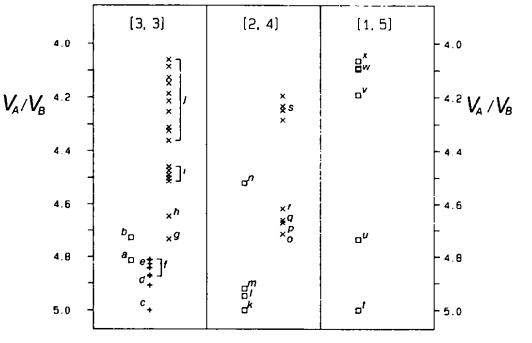

Fig. 8. V_A/V_B-cation charge $[z_A,z_B]$–symmetry correlations for known perovskite structures with tilted octahedra. Structures have been determined at room temperature, except where otherwise indicated, with V_A/V_B values calculated previously (Thomas & Beitollahi, 1994; Thomas, 1996). Space-group symmetry is denoted by the following symbols: □: rhombohedral $R3c$; +: rhombohedral $R\bar{3}c$; x: orthorhombic *Pnma*. Structures are represented by alphabetical characters as follows: (*a*) $NdAlO_3$; (*b*) $BiFeO_3$; (*c*) $PrAlO_3$; (*d*) $LaCuO_3$; (*e*) $NdAlO_3$; (*f*) $LaCoO_3$ (six structures; 4–1248 K); (*g*) $SmAlO_3$; (*h*) $LaFeO_3$; (*i*) (in descending V_A/V_B ratio) $NdFeO_3$, $HoNiO_3$, $PrFeO_3$, $SmNiO_3$, $PrFeO_3$ and $YAlO_3$; (*j*) lanthanide ferrites, $LnFeO_3$, from $SmFeO_3$ ($V_A/V_B = 4.362$) to $LuFeO_3$ ($V_A/V_B = 4.060$); (*k*) $Pb(Zr_{0.75}Ti_{0.25})O_3$; (*l*) and (*m*) $Pb(Zr_{0.9}Ti_{0.1})O_3$; (*n*) $HgTiO_3$; (*o*) $BaPrO_3$; (*p*) $BaCeO_3$; (*q*) $SrZrO_3$; (*r*) $CaTiO_3$; (*s*) $MgSiO_3$ at various hydrostatic pressures: $V_A/V_B = 4.284$ at 0 GPa (Horiuchi, Ito & Weidner, 1987) to 4.195 at 9.6 GPa (Kudoh, Ito & Takeda, 1987); (*t*) $KNbO_3$; (*u*) $NaNbO_3$ (123 K); (*v*) $LiReO_3$; (*w*) $LiTaO_3$, $LiUO_3$; (*x*) $LiNbO_3$.

Calculations of electrostatic energy for rhombohedral $BiFeO_3$ and $Pb(Zr_{0.9}Ti_{0.1})O_3$ also support this conclusion (Thomas & Beitollahi, 1994).

Within the [2,4]-column, there is again a transition to orthorhombic *Pnma* at lower V_A/V_B ratios, with the exception of $HgTiO_3$ (point *n*). Here, the adoption of rhombohedral symmetry is probably related to the unique coordination chemistry of mercury, in which three short bonds are formed with oxygen ions (Sleight & Prewitt, 1973). $MgSiO_3$ is the [2,4]-perovskite with the smallest V_A/V_B ratio, this being an important mineral within the Earth's mantle. Upon application of hydrostatic pressure, V_A/V_B falls from 4.284 at 0 GPa (Horiuchi, Ito & Weidner, 1987) to 4.195 at 9.6 GPa (Kudoh, Ito & Takeda, 1987). Thus, $EuFeO_3$, with its V_A/V_B ratio of 4.324, would be a [3,3]-analogue of $MgSiO_3$ at 0 GPa. The corresponding analogue of $MgSiO_3$ at 9.6 GPa would be $HoFeO_3$, with a V_A/V_B ratio of 4.187. It follows that larger pressures can be simulated chemically by exploiting the lanthanide contraction. For example, $LuFeO_3$ has the smallest V_A/V_B ratio of 4.060. This is equivalent to the polyhedral volume ratio $MgSiO_3$ would be expected to have at a pressure of approximately 24 GPa, assuming a linear extropolation of the variation of V_A/V_B with pressure between 0 and 9.6 GPa. Such lanthanide ferrites (points *j* in Fig. 8) would, therefore, be of use in laboratory simulations of $MgSiO_3$ as it occurs in the Earth's mantle, at hydrostatic pressures of the order 20 GPa. Deformation experiments at high temperatures and pressures of $MgSiO_3$ and its lanthanide ferrite analogues would thus be of considerable mineralogical interest.

All [1,5]-perovskites are stabilized in polar phases *R*3*m* and *R*3*c*, pointing to the significant dipole–dipole contribution to the lattice energy. It is to be noted that $KNbO_3$ and $NaNbO_3$ are unstable against polymorphic phase changes. In the case of $KNbO_3$, ferroelectric phases of orthorhombic and tetragonal symmetry are stabilized at higher temperatures. Point *u* in Fig. 8 refers to $NaNbO_3$ in its rhombohedral structure at 123 K. However, this compound is richly polymorphic, showing six alternative symmetries (Thomas, 1996). The room-temperature structure has the orthorhombic space group *Pbcm*, with significant displacements of *A* and *B* ions from their polyhedral centres (Thomas, 1996). These, together with the observed antiferroelectric properties, provide further evidence of the importance of dipole–dipole interactions in determining the structures of [1,5]-perovskites. $LiNbO_3$ has the minimum V_A/V_B ratio of 4.065 and, in contrast to $KNbO_3$ and $NaNbO_3$, is stable against polymorphic modifications. It undergoes a straightforward transition to non-polar $R\bar{3}c$ symmetry at the very high Curie point of 1483 K.

In general, considerations of ionic charge and the structural geometry resulting from different ionic sizes are sufficient to rationalize the symmetries of the structures adopted by different compositions. Exceptions to this generalization are found in compositions with strong dipole–dipole interactions or particular coordination chemistries (as for oxygen-coordinated Zr^{4+}, Pb^{2+} and Hg^{2+} ions, for example). Here, there is a strong tendency towards polymorphism. Further work is required to understand the delicate energy balances between the alternative modifications.

References

Hammond, C. (1990). *Introduction to Crystallography*, p. 91. Oxford University Press.

Horiuchi, H., Ito, E. & Weidner, D. J. (1987). *Am. Mineral.* **72**, 357–360.

Kudoh, Y., Ito, E. & Takeda, H. (1987). *Phys. Chem. Miner.* **14**, 350–354.

Megaw, H. D. & Darlington, C. N. W. (1975). *Acta Cryst.* A**31**, 161–173.

Michel, C., Moreau, J. M. & James, W. J. (1971). *Acta Cryst.* B**27**, 501–503.

Sleight, A. W. & Prewitt, C. T. (1973). *J. Solid State Chem.* **6**, 509–512.

Thomas, N. W. (1996). *Acta Cryst.* B**52**, 16–31

Thomas, N. W. & Beitollahi, A. (1994). *Acta Cryst.* B**50**, 549–560.